Some Reactions of $[Os_3(\mu\text{-}H)_3(CO)_9(\mu_3\text{-}CX)]$ (X = OMe or Cl): The Formation of C–N and C–P Bonds†

Brian F. G. Johnson, Fernando J. Lahoz, Jack Lewis,* Neville D. Prior, Paul R. Raithby and Wing-Tak Wong

University Chemical Laboratory, Lensfield Road, Cambridge CB2 1EW, UK

The reaction of $[Os_3(\mu\text{-}H)_3(CO)_9(\mu_3\text{-}COMe)]$ **1** with a slight excess of the sterically hindered base 1,8-diazabicyclo[5.4.0]undec-7-ene (dbu) affords the anion $[Os_3(\mu\text{-}H)_2(CO)_9(\mu_3\text{-}COMe)]^-$ **3** which has been isolated as its $N(PPh_3)_2^+$ salt in high yield. Treatment of **3** with $[Au(PPh_3)]Cl$ in the presence of $TlPF_6$ gives $[Os_3(\mu\text{-}H)_2(\mu\text{-}AuPPh_3)(CO)_9(\mu_3\text{-}COMe)]$ **4** in high yield. The cluster $[Os_3(\mu\text{-}H)_3(CO)_9(\mu_3\text{-}CCl)]$ **2** reacts with 1 equivalent of dbu to produce a highly unstable species thought to be $[Os_3(\mu\text{-}H)_2(CO)_9(\mu_3\text{-}CCl)]^-$ which, in the presence of excess of dbu, gives the yellow compound $[Os_3(\mu\text{-}H)_2(CO)_9(\mu_3\text{-}CN_2C_9H_{16})]$ **5** in good yield. This reaction has been found to be general and the reaction of **2** with 1 equivalent of dbu in the presence of a twenty-fold excess of the required nucleophile Y gives the compounds $[Os_3(\mu\text{-}H)_2(CO)_9(\mu_3\text{-}CY)]$ (Y = pyridine **6**, quinoline **7**, isoquinoline **8** or trimethyl phosphite **9**). The molecular structures of complexes **4**, **5**, **7** and **9** have been established by single-crystal X-ray analysis. Both structural features and spectroscopic data for compounds **4**–**9** are consistent with a zwitterionic formulation of these species. Complex **7** exhibits a strong negative solvatochromism in a wide range of organic solvents, suggesting a less-polar excited state upon photoexcitation.

The chemistry of alkylidyne clusters $[M_3(\mu\text{-}H)_3(CO)_9(\mu_3\text{-}CX)]$ of the iron triad is currently under active investigation.[1] The reactivity of these compounds has been shown to involve (*i*) modification of the alkylidyne substituent,[2] (*ii*) ligand substitution on the metal centres,[3] (*iii*) protonation and deprotonation,[4] (*iv*) alkyne insertion into the M–CX bond[5] and (*v*) reductive elimination of CX groups.[6]

The alkylidyne substituents of $[M_3(\mu\text{-}H)_n(CO)_9(\mu_3\text{-}CX)]$ (M = Ru or Os, n = 2 or 3) are mainly confined to carbon-, oxygen- or halogen-containing groups.[2] We now report a general synthetic route to a new class of triosmium alkylidyne clusters with nitrogen or phosphorus substituents on the apical carbon atom.

Results and Discussion

The reaction of $[Os_3(\mu\text{-}H)_3(CO)_9(\mu_3\text{-}COMe)]$ **1** with a slight excess of the sterically hindered base 1,8-diazabicyclo[5.4.0]-undec-7-ene (dbu) (1.2 equivalents) in CH_2Cl_2 affords the anionic cluster $[Os_3(\mu\text{-}H)_2(CO)_9(\mu_3\text{-}COMe)]^-$ **3** which can be isolated as its $N(PPh_3)_2^+$ salt in high yield. Treatment of **3** with a slight excess of $[Au(PPh_3)]Cl$ in the presence of $TlPF_6$ in CH_2Cl_2 at room temperature gives $[Os_3(\mu\text{-}H)_2(\mu\text{-}AuPPh_3)(CO)_9(\mu_3\text{-}COMe)]$ **4** in good yield. The cluster $[Os_3(\mu\text{-}H)_3(CO)_9(\mu_3\text{-}CCl)]$ **2** reacts with 1 equivalent of dbu to produce a yellow species, thought to be $[Os_3(\mu\text{-}H)_2(CO)_9(\mu_3\text{-}CCl)]^-$ which decomposes rapidly even at low temperature (−50 °C). However, in the presence of excess of dbu, a yellow compound $[Os_3(\mu\text{-}H)_2(CO)_9(\mu_3\text{-}CN_2C_9H_{16})]$ **5** can be isolated in good yield. This observation on the $[Os_3(\mu\text{-}H)_3(CO)_9(\mu_3\text{-}CCl)]$–dbu system led us to a general route for the preparation of the species $[Os_3(\mu\text{-}H)_2(CO)_9(\mu_3\text{-}CY)]$ (Y = Lewis base). The reaction of $[Os_3(\mu\text{-}H)_3(CO)_9(\mu_3\text{-}CCl)]$ with 1 equivalent of dbu, in the presence of a twenty-fold excess of the required nucleophile (Y), gives the compound $[Os_3(\mu\text{-}H)_2(CO)_9(\mu_3\text{-}CY)]$ in moderate to good yields. It is assumed that the nucleophile used will have a higher nucleophilicity than dbu, hence limiting the formation of **5**. Utilising this synthetic pathway, we have been able to introduce a variety of substituents (pyridine, quinoline, isoquinoline and trimethyl phosphite) at the apical carbon atom of the alkylidyne cluster. However, attempts to replace the dbu with a more sterically hindered base such as 1,8-bis(dimethylamino)naphthalene (proton sponge) failed to give any reaction. Using KOH–MeOH as the deprotonating agent with **2** gives **3** in moderate yield. These reactions are summarised in Scheme 1. The detailed mechanism has not been established. However, it is believed that the anionic species generated by deprotonation of **2** may dissociate to give a chloride ion and a highly reactive transient species '$Os_3(\mu\text{-}H)_2(CO)_9(\mu_3\text{-}C)$' which is trapped by the nucleophile (Y) to give the product $[Os_3(\mu\text{-}H)_2(CO)_9(\mu_3\text{-}CY)]$ (Scheme 2).

The spectroscopic data (IR, ^1H NMR and mass spectroscopic) for the new compounds are summarised in Table 1. Compounds **5**–**9**, as expected, have many common spectral features. They have very similar solution IR spectral patterns in the carbonyl stretching absorption region suggesting that they are isostructural. Although they are neutral molecules, the values of the carbonyl stretching frequencies are all at lower wavenumber compared with those of **1** and **4**. This may be taken as an indication of the electron richness of the metal cores in this class of complexes. Compounds **5**–**8** all show a singlet and **9** shows a doublet in the hydride region of the ^1H NMR spectrum in the range δ −18 to −21. The proton signals due to the organic moieties in **5**–**9** are fully consistent with the solid-state structures (in the case of **5**, **7** and **9**) or the proposed structures (**6** and **8**). However, no attempt was made fully to assign all these signals.

The molecular structures of complexes **4**, **5**, **7** and **9** have been established by single-crystal X-ray analyses. That of **4** is shown in Fig. 1 and selected bond distances and angles are presented in Table 2. The methoxymethylidyne ligand μ_3 bridges the osmium triangle and the Os–C (alkylidyne) bond lengths are essentially equivalent. Two carbonyl ligands make relatively short contacts with the Au atom [Au···C(13) 2.76, Au···C(32) 2.70 Å]. A similar observation has been reported for the analogous ruthenium compound.[7] Recent molecular orbital

† *Supplementary data available:* see Instructions for Authors, *J. Chem. Soc., Dalton Trans.*, 1992, Issue 1, pp. xx–xxv.

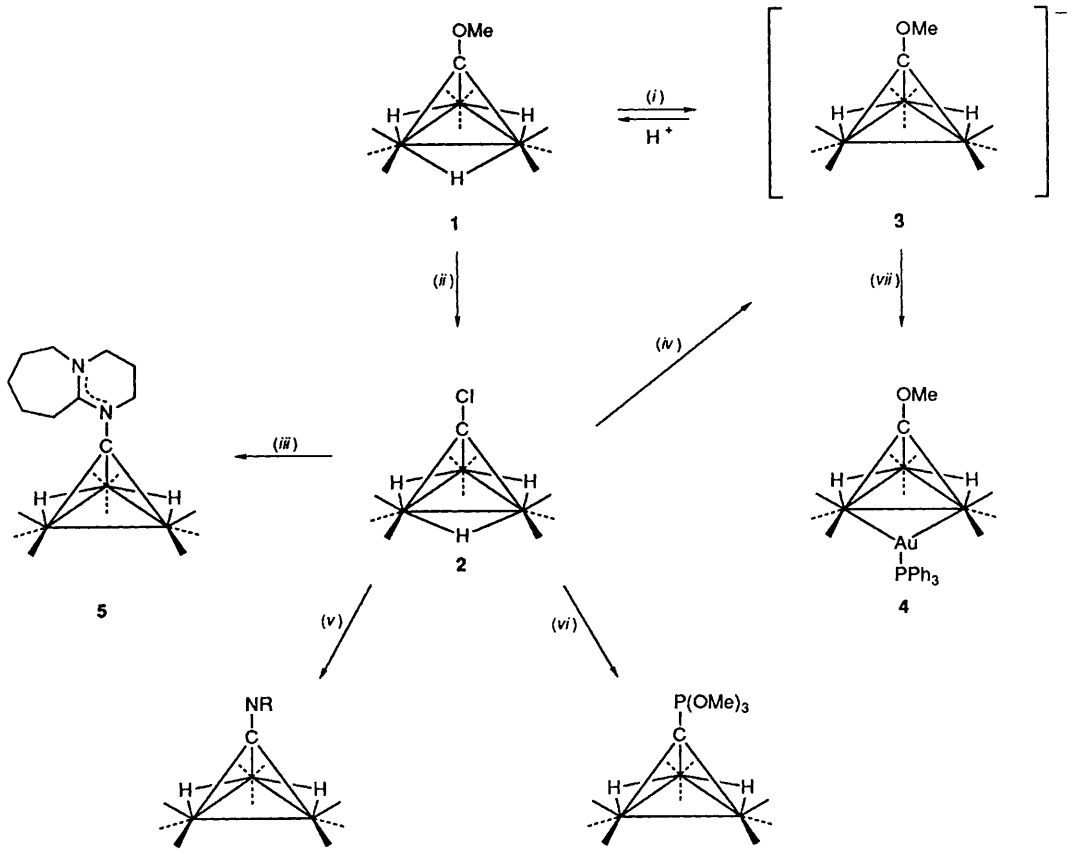

Scheme 1 Reactions of $[Os_3(\mu\text{-}H)_3(CO)_9(\mu_3\text{-}COMe)]$ **1** and related compounds. (*i*) dbu; (*ii*) BCl_3; (*iii*) excess of dbu; (*iv*) KOH–MeOH; (*v*) amine–dbu; (*vi*) $P(OMe)_3$–dbu; (*vii*) $[Au(PPh_3)]Cl$–$TlPF_6$

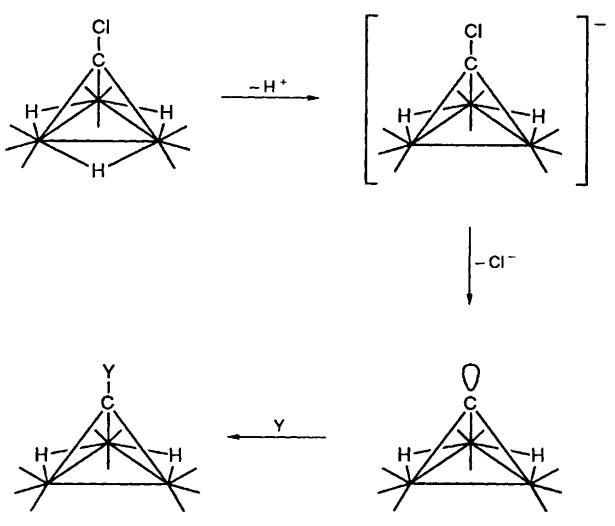

Scheme 2 Proposed mechanism for the formation of $[Os_3(\mu\text{-}H)_2(CO)_9(\mu_3\text{-}CY)]$ (Y = Lewis base) from $[Os_3(\mu\text{-}H)_3(CO)_9(\mu_3\text{-}CCl)]$

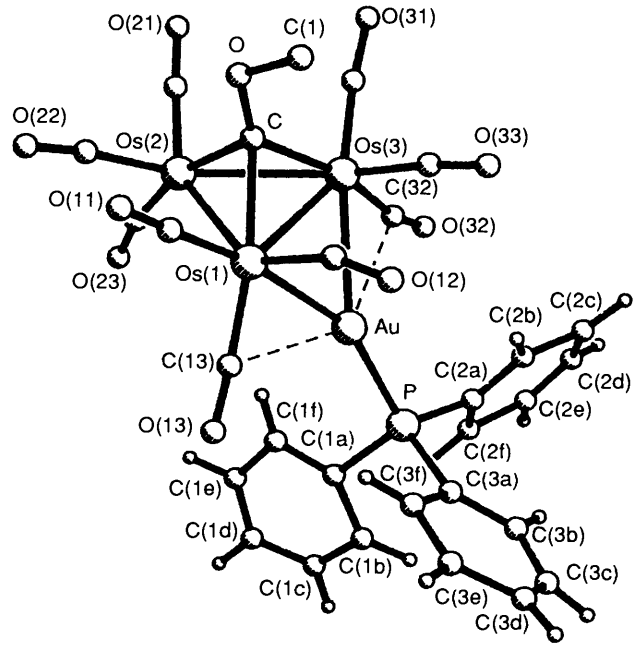

Fig. 1 The molecular structure of $[Os_3(\mu\text{-}H)_2(\mu\text{-}AuPPh_3)(CO)_9(\mu_3\text{-}COMe)]$ **4**

calculations by the Fenske–Hall method on $[Fe_3(CO)_{10}(\mu_3\text{-}CH)(CuPH_3)]$ have shown that the close contacts of carbonyls to the Cu atom are not a consequence of electronic effects, but rather of steric factors.[8] The molecular structures of **5**, **7** and **9**, as shown by X-ray analyses, all consist of a triosmium alkylidyne metal core with the nucleophiles [dbu in **5**, quinoline in **7** and $P(OMe)_3$ in **9**] bonded to the μ_3-bridging alkylidyne carbon atom. The structure of **5** shows the dbu ligand to have co-ordinated *via* the less sterically hindered, yet less basic, nitrogen atom. This result is almost certainly derived from unfavourable steric interactions between the incoming dbu ligand and the pseudo-equatorial carbonyl ligands, pointing towards the co-ordinated dbu. The molecular structure and space-filling model of **5** are shown in Figs. 2 and 3 respectively. The double bond originally present in the dbu molecule appears to be delocalised over N(2)–C(108)–N(1), as shown by the bond angle around C(108) and the equality of the N(2)–C(108) and N(1)–C(108) bond lengths, see Table 3. The hydride atoms of **5**, evident from the ^1H NMR spectrum, cannot be located by X-ray analysis. However, potential-energy calculations suggested that one bridges the Os(1)–Os(3) edge and the other the Os(2)–Os(3)

Table 1 Spectroscopic data for new compounds of the type $[Os_3(\mu\text{-}H)_2(CO)_9(\mu_3\text{-}CX)]$

Compound	IR, ν(CO)/cm^{-1}	^{1}H NMR[a]	Mass spectrum, m/z[b]
3 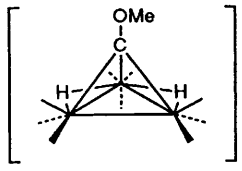	2068w, 2028s, 1997vs, 1970w, 1952m, 1924m	7.74 [30 H, m, $N(PPh_3)_2^+$] 3.70 (3 H, s, OMe)	—
4 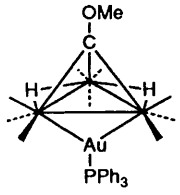	2093m, 2057s, 2039vs, 2009m, 1997m, 1964m	7.48 (15 H, m, Ph) 3.89 (3 H, s, OMe) −20.35 [2 H, d, ^3J(PH) = 1.5, OsH]	1332 (1332)
5 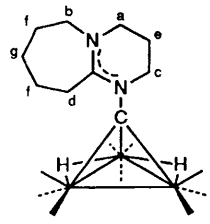	2080m, 2046vs, 2014vs, 1999m, 1974s, 1941m, 1924m	4.18 (2 H, m, H_a) 3.88 (2 H, br, H_b) 3.54 (2 H, m, H_c) 3.37 [2 H, t, $J(H_dH_f)$ = 6, H_d)] 2.13 (2 H, m, H_e) 1.83 (4 H, br, H_f) 1.75 (2 H, br, H_g) −18.95 (2 H, s, OsH)	994 (994)
6 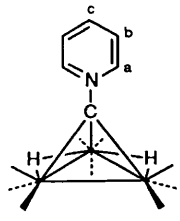	2091m, 2055vs, 2024vs, 2000m, 1983s, 1950m, 1935m	9.69 [2 H, dd, $J(H_aH_b)$ = 6.9, $J(H_aH_c)$ = 1.2, H_a] 8.26 [1 H, tt, $J(H_cH_b)$ = 7.5, $J(H_cH_a)$ = 1.2, H_c]	921 (921)
7 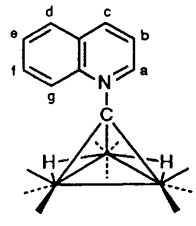	2090m, 2055vs, 2023vs, 2000m, 1983s, 1950m, 1935m	11.05 [1 H, dd, $J(H_aH_b)$ = 6.1, $J(H_aH_c)$ = 1.2, H_a] 10.02 [1 H, d, $J(H_gH_f)$ = 9.1, H_g] 8.92 [1 H, d, $J(H_cH_b)$ = 8.2, H_c] 8.17 (2 H, m, H_f and H_d) 7.82 [1 H, dt, $J(H_cH_d)$ = $J(H_cH_f)$ = 7.9, $J(H_eH_g)$ = 0.7, H_e] 7.43 [1 H, dd, $J(H_cH_a)$ = 6.1, $J(H_bH_c)$ = 8.2, H_b] −18.58 (2 H, s, OsH)	973 (973)
8 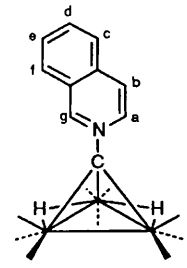	2090m, 2054vs, 2024vs, 2001m, 1982s, 1950m, 1934m	10.40 [1 H, d, $J(H_gH_a)$ = 1.3, H_g] 9.18 [1 H, dd, $J(H_aH_b)$ = 7.0, $J(H_aH_g)$ = 1.3, H_a] 8.20 [1 H, d, $J(H_fH_c)$ = 8.3, H_f] 8.07 (1 H, m, H_d or H_e) 7.98 [1 H, d, $J(H_cH_d)$ = 7.7, H_c] 7.84 (1 H, m, H_d or H_e) 7.80 [1 H, d, $J(H_bH_a)$ = 7.0, H_b] −18.81 (2 H, s, OsH)	973 (973)
9 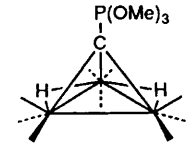	2099m, 2060vs, 2030vs, 2015m, 1981s, 1961m, 1945m	3.97 [9 H, d, ^3J(PH) = 10.5, OMe] −20.43 [2 H, d, ^3J(PH) = 2.6, OsH]	966 (966)

[a] J values in Hz. [b] Calculated values (based on ^{187}Os) given in parentheses.

edge. These two edges (average 2.879 Å) are significantly longer than the Os(1)–Os(2) bond [2.739(1) Å]. This is consistent with the general observation that M–M distances are increased when bridged by a hydride atom.[9] So far as we are aware, **5** is the only example of a dbu derivative of a carbonyl cluster that has been structurally characterised. The molecular structures of com-

Table 2 Selected bond lengths (Å) and angles (°) for $[Os_3(\mu\text{-}H)_2(\mu\text{-}AuPPh_3)(CO)_9(\mu_3\text{-}COMe)]$ **4**

Os(1)–Os(2)	2.902(3)	Au–P	2.30(1)
Os(1)–Os(3)	2.886(3)	C–O	1.32(5)
Os(2)–Os(3)	2.889(4)	O–C(1)	1.43(8)
Os(1)–Au	2.740(3)	Au ··· C(13)	2.76(4)
Os(3)–Au	2.770(2)	Au ··· C(32)	2.70(4)
Os(2)–C	2.11(4)	Os–C(carbonyl)	1.74–1.94(5)
Os(1)–C	2.20(4)	C–O(carbonyl)	1.14–1.25(8)
Os(3)–C	2.11(5)		
Os(2)–Os(1)–Os(3)	59.9(1)	Os(2)–C–O	123(4)
Os(1)–Os(2)–Os(3)	59.8(1)	Os(3)–C–O	135(4)
Os(1)–Os(3)–Os(2)	60.3(1)	C–O–C(1)	115(4)
Os(1)–Au–Os(3)	63.2(1)	Au–P–C(1a)	112(2)
Os(3)–Os(1)–Au	58.9(1)	Au–P–C(2a)	113(2)
Os(1)–Os(3)–Au	57.9(1)	Au–P–C(3a)	113(2)
Os(1)–C–Os(2)	85(2)	C(1a)–P–C(2a)	107(2)
Os(1)–C–Os(3)	84(2)	C(1a)–P–C(3a)	107(2)
Os(2)–C–Os(3)	87(2)	C(2a)–P–C(3a)	104(3)
Os(1)–C–O	126(3)	Os–C–O(carbonyl)	160–178(4)

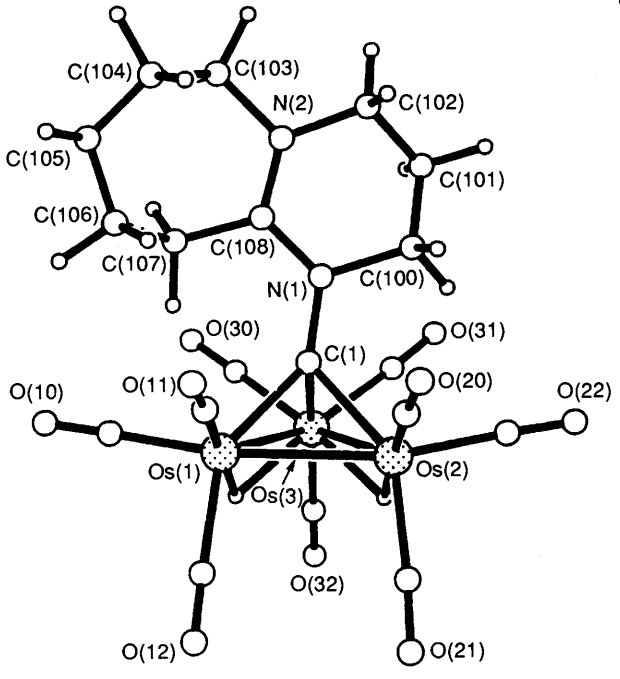

Fig. 2 The molecular structure of $[Os_3(\mu\text{-}H)_2(CO)_9(\mu_3\text{-}CN_2C_9H_{16}]$ **5**

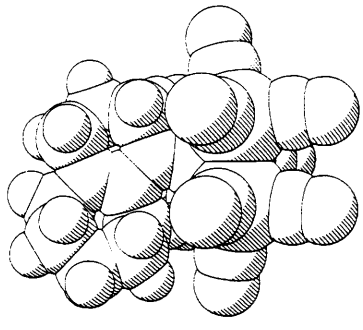

Fig. 3 Space-filling drawing of complex **5**

plexes **7** and **9** are shown in Fig. 4 and 5, respectively, and selected bond parameters are in Tables 4 and 5. The basic metal cluster core units are essentially identical to that observed in **5**. The average non-bridged Os–Os bond length for **5**, **7** and **9** [2.746(1) Å] is notably shorter than the 2.887(3) Å observed in $[Os_3(CO)_{12}]$,[10] whilst the mean value of 2.881(6) Å for the

Table 3 Selected bond lengths (Å) and angles (°) for $[Os_3(\mu\text{-}H)_2(CO)_9(\mu_3\text{-}CN_2C_9H_{16})]$ **5**

Os(1)–Os(2)	2.739(1)	N(2)–C(102)	1.48(3)
Os(1)–Os(3)	2.883(1)	N(2)–C(108)	1.35(2)
Os(2)–Os(3)	2.875(1)	N(2)–C(103)	1.47(3)
Os(1)–C(1)	2.12(2)	C(103)–C(104)	1.51(4)
Os(2)–C(1)	2.14(2)	C(104)–C(105)	1.42(5)
Os(3)–C(1)	2.14(2)	C(105)–C(106)	1.41(5)
C(1)–N(1)	1.44(2)	C(106)–C(107)	1.54(4)
N(1)–C(100)	1.55(3)	C(107)–C(108)	1.48(3)
N(1)–C(108)	1.35(2)	Os–C(carbonyl)	1.83–1.97(3)
C(100)–C(101)	1.45(4)	C–O(carbonyl)	1.10–1.22(4)
C(101)–C(102)	1.44(5)		
Os(2)–Os(1)–Os(3)	61.4(1)	C(100)–C(101)–C(102)	115(3)
Os(1)–Os(2)–Os(3)	61.7(1)	N(2)–C(102)–C(101)	108(2)
Os(1)–Os(3)–Os(2)	56.8(1)	C(102)–N(2)–C(103)	114(2)
Os(1)–C(1)–Os(2)	80.1(6)	C(102)–N(2)–C(108)	125(2)
Os(1)–C(1)–Os(3)	85.3(7)	C(103)–N(2)–C(108)	122(2)
Os(3)–C(1)–Os(3)	84.3(7)	N(2)–C(103)–C(104)	113(2)
Os(1)–C(1)–N(1)	138(1)	C(103)–C(104)–C(105)	120(3)
Os(2)–C(1)–N(1)	125(1)	C(104)–C(105)–C(106)	118(3)
Os(3)–C(1)–N(1)	126(1)	C(105)–C(106)–C(107)	116(3)
C(1)–N(1)–C(100)	116(2)	N(1)–C(108)–C(107)	119(2)
C(1)–N(1)–C(108)	127(2)	N(2)–C(108)–C(107)	119(2)
C(100)–N(1)–C(108)	117(2)	N(1)–C(108)–N(2)	122(2)
N(1)–C(100)–C(101)	113(2)	Os–C–O(carbonyl)	174–180(3)

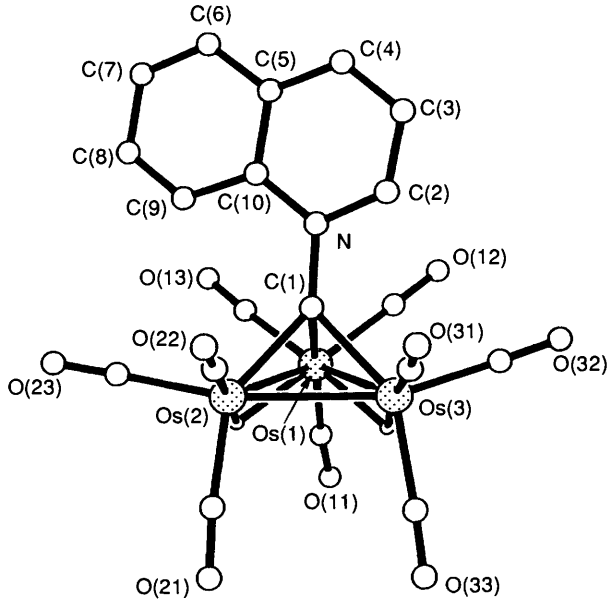

Fig. 4 The molecular structure of $[Os_3(\mu\text{-}H)_2(CO)_9(\mu_3\text{-}CNC_9H_7)]$ **7**

hydride-bridged Os–Os distance is similar to that observed in $[Os_3(CO)_{12}]$. The metal–alkylidyne carbon bond distances are typical of those in osmium alkylidyne clusters already structurally characterised.[2] The best bonding description of these species is a charge-separated, zwitterionic formulation as shown in Fig. 6. This formulation is consistent with the solution IR spectra of these compounds which show unusually low carbonyl stretching frequencies for neutral triosmium carbonyl clusters. Furthermore, the ^{13}C NMR spectrum of **6** showed an upfield resonance for the methylidyne carbon (δ 29.9) in CD_2Cl_2 at room temperature. This value is similar to that reported for the compound $[Os_3(\mu\text{-}H)_2(CO)_9(\mu_3\text{-}CCO)]$.[11] However, the signals of the methylidyne carbon in $[Os_3(\mu\text{-}H)_3(CO)_9(\mu_3\text{-}CX)]$ (X = H, Me, Ph, OMe, F, Cl or Br) appear in the region δ 110–220.[2,12]

Compounds **5**–**9** show a variety of colours (**5**, yellow; **6**, red; **7**, purple; **8**, deep red; **9**, creamy yellow) in the solid state. Molecular orbital calculations by the Fenske–Hall method show that the highest occupied molecular orbital (HOMO) of

Table 4 Selected bond lengths (Å) and angles (°) for $[Os_3(\mu\text{-}H)_2(CO)_9(\mu_3\text{-}CNC_9H_7)]$ **7**

Os(1)–Os(2)	2.888(1)	C(3)–C(4)	1.36(3)
Os(1)–Os(3)	2.871(1)	C(4)–C(5)	1.37(3)
Os(2)–Os(3)	2.743(1)	C(5)–C(6)	1.42(3)
Os(1)–C(1)	2.16(2)	C(5)–C(10)	1.44(3)
Os(2)–C(1)	2.13(2)	C(6)–C(7)	1.34(3)
Os(3)–C(1)	2.11(2)	C(7)–C(8)	1.39(3)
C(1)–N	1.44(3)	C(8)–C(9)	1.34(3)
N–C(2)	1.36(2)	C(9)–C(10)	1.40(3)
N–C(10)	1.38(2)	Os–C(carbonyl)	1.82–1.97(2)
C(2)–C(3)	1.38(3)	C–O(carbonyl)	1.13–1.21(3)
Os(2)–Os(1)–Os(3)	56.9(1)	C(2)–C(3)–C(4)	118(2)
Os(1)–Os(2)–Os(3)	61.2(1)	C(3)–C(4)–C(5)	121(2)
Os(1)–Os(3)–Os(2)	61.9(1)	C(4)–C(5)–C(6)	124(2)
Os(1)–C(1)–Os(2)	84.8(7)	C(4)–C(5)–C(10)	119(2)
Os(1)–C(1)–Os(3)	84.6(7)	C(6)–C(5)–C(10)	117(2)
Os(2)–C(1)–Os(3)	80.8(7)	C(5)–C(6)–C(7)	122(2)
Os(1)–C(1)–N	124(1)	C(6)–C(7)–C(8)	121(2)
Os(2)–C(1)–N	136(1)	C(7)–C(8)–C(9)	119(2)
Os(3)–C(1)–N	130(1)	C(8)–C(9)–C(10)	124(2)
C(1)–N–C(2)	117(2)	N–C(10)–C(5)	120(2)
C(1)–N–C(10)	125(2)	N–C(10)–C(9)	123(2)
C(2)–N–C(10)	117(2)	C(5)–C(10)–C(9)	117(2)
N–C(2)–C(3)	124(2)	Os–C–O(carbonyl)	175–179(3)

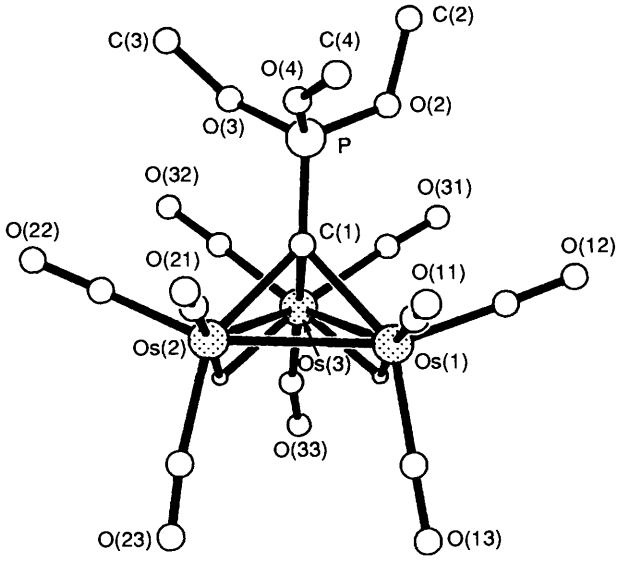

Fig. 5 The molecular structure of $[Os_3(\mu\text{-}H)_2(CO)_9\{\mu_3\text{-}CP(OMe)_3\}]$ **9**

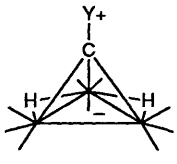

Fig. 6 Zwitterionic formulation for $[Os_3(\mu\text{-}H)_2(CO)_9(\mu_3\text{-}CY)]$ (Y = Lewis base)

these compounds is largely metal based (*ca.* 70%), whilst the lowest unoccupied molecular orbital (LUMO) is mostly dominated by the organic moiety.[13] The intense colour of these compounds undoubtedly arises from a strong absorption due to a metal-to-ligand charge-transfer (m.l.c.t.) transition. A study of complex **7** in a variety of organic solvents by UV/VIS spectroscopy demonstrated that the m.l.c.t. transition band displays negative solvatochromism. The spectra in acetone, dichloromethane and hexane are shown in Fig. 7, whilst optical spectral parameters for a range of solvents are summarised in Table 6. This phenomenon has been recently observed in a series of mononuclear transition-metal carbonyl complexes.[14] Solvatochromism is only seen if the solvent–solute interaction in the ground state shows a significant difference from that in the excited state of the molecule. Compound **7** has a ligand–metal framework in which the bonding is polarised in the ground state, probably due to a dominating σ donation from the nitrogen heterocycle. However, on m.l.c.t. excitation, this polarisation will be either reduced, compensated, or even over compensated for, by transfer of an electron from the metal-based orbital (HOMO) to the empty π* orbital of the organic

Table 5 Selected bond lengths (Å) and angles (°) for $[Os_3(\mu\text{-}H)_2(CO)_9\{\mu_3\text{-}CP(OMe)_3\}]$ **9**

Os(1)–Os(3)	2.757(2)	P–O(3)	1.51(3)
Os(1)–Os(3)	2.884(2)	P–O(4)	1.50(5)
Os(2)–Os(3)	2.885(2)	O(2)–C(2)	1.46(7)
Os(1)–C(1)	2.10(2)	O(3)–C(3)	1.37(6)
Os(2)–C(1)	2.10(3)	O(4)–C(4)	1.33(9)
Os(3)–C(1)	2.16(4)	Os–C(carbonyl)	1.84–1.97(6)
P–C(1)	1.65(4)	C–O(carbonyl)	1.09–1.21(9)
P–O(2)	1.53(3)		
Os(2)–Os(1)–Os(3)	61.5(1)	C(1)–P–O(3)	111(2)
Os(1)–Os(2)–Os(3)	61.4(1)	C(1)–P–O(4)	114(2)
Os(1)–Os(3)–Os(2)	57.1(1)	O(2)–P–O(3)	107(2)
Os(1)–C(1)–Os(2)	82(1)	O(2)–P–O(4)	111(3)
Os(1)–C(1)–Os(3)	85(1)	O(3)–P–O(4)	103(2)
Os(2)–C(1)–Os(3)	85(1)	P–O(2)–C(2)	128(2)
Os(1)–C(1)–P	131(2)	P–O(3)–C(3)	145(5)
Os(2)–C(1)–P	132(1)	P–O(4)–C(4)	150(4)
Os(3)–C(1)–P	125(2)	Os–C–O(carbonyl)	170–178(4)
C(1)–P–O(2)	110(2)		

Table 6 Optical spectral parameters for $[Os_3(\mu\text{-}H)_2(CO)_9(\mu_3\text{-}CNC_9H_7)]$ **7** in various organic solvents

Solvent	Colour	λ_{max}/nm	$10^5\varepsilon/m^2\,mol^{-1}$ ±0.5
Hexane	Green	620	4.0
Carbon tetrachloride	Green	611	3.7
Chloroform	Blue	578	4.3
Toluene	Blue	577	4.2
Dichloromethane	Purple	566	4.4
Diethyl ether	Purple	565	4.4
1,2-Dichloroethane	Purple	562	4.5
Butanol	Purple	559	4.4
Ethanol	Purple	552	5.0
Ethyl acetate	Lilac	550	4.2
Tetrahydrofuran	Lilac	550	4.4
Ethyl methyl ketone	Pink	541	4.3
Methanol	Red	540	4.4
Acetone	Red	536	4.0

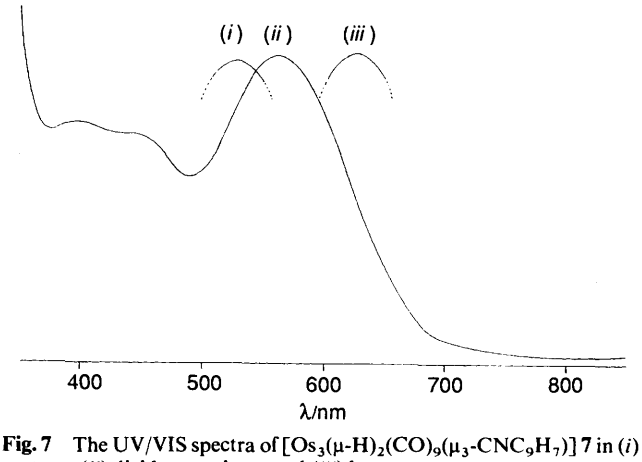

Fig. 7 The UV/VIS spectra of $[Os_3(\mu\text{-}H)_2(CO)_9(\mu_3\text{-}CNC_9H_7)]$ **7** in (*i*) acetone, (*ii*) dichloromethane and (*iii*) hexane

Table 7 Crystal data and data-collection parameters* for the structures of $[Os_3(\mu\text{-}H)_2(\mu\text{-}AuPPh_3)(CO)_9(\mu_3\text{-}COMe)]$ **4**, $[Os_3(\mu\text{-}H)_2(CO)_9(\mu_3\text{-}CN_2C_9H_{16})]$ **5**, $[Os_3(\mu\text{-}H)_2(CO)_9(\mu_3\text{-}CNC_9H_7)]$ **7** and $[Os_3(\mu\text{-}H)_2(CO)_9\{\mu_3\text{-}CP(OMe)_3\}]$ **9**

	4	**5**	**7**	**9**
Molecular formula	$C_{29}H_{20}AuO_{10}Os_3P$	$C_{19}H_{18}N_2O_9Os_3$	$C_{19}H_9NO_9Os_3$	$C_{13}H_{11}O_{12}Os_3P$
M	1327.0	988.94	956.86	960.81
Crystal colour, habit	Yellow rectangular plates	Yellow rectangular plates	Purple blocks	Pale yellow blocks
Crystal size (mm)	0.18 × 0.22 × 0.45	0.04 × 0.30 × 0.31	0.23 × 0.2 × 0.34	0.08 × 0.09 × 0.15
Space group	$P2_1/c$	$P2_1/n$	$P2_1/c$	$C2/c$
a/Å	13.424(6)	9.182(2)	9.095(5)	32.627(5)
b/Å	17.026(4)	17.911(5)	11.859(3)	8.481(4)
c/Å	15.845(6)	14.798(4)	20.423(4)	18.814(4)
β/°	110.84(1)	100.28(2)	100.63(2)	124.49(1)
U/Å^3	3385(2)	2394(3)	2165(3)	4920(4)
Z	4	4	4	8
D_c/g cm^{-3}	2.604	2.743	2.935	2.974
F(000)	2384	1784	1720	3424
μ(Mo-Kα)/cm^{-1}	156.55	159.20	176.03	178.37
Diffractometer	Nicolet R3m/v	Stoe–Siemens	Stoe–Siemens	Stoe–Siemens
2θ Range/°	5–45	5–50	5–45	5–45
Scan speed/° min^{-1}	3.00–29.30	1.50–6.00	1.50–6.00	1.50–6.00
Scan range (ω)/°	1.40 plus Kα separation	1.20 plus Kα separation	1.20 plus Kα separation	1.20 plus Kα separation
Reflections measured	4691	4539	3089	3097
Unique reflections	4153	4214	2827	2803
Observed reflections (criterion)	2504 [$F > 3\sigma(F)$]	3493 [$F > 4\sigma(F)$]	2384 [$F > 4\sigma(F)$]	1842 [$F > 4\sigma(F)$]
Absorption correction	ψ-Scan method	Numerical method	ψ-Scan method	Numerical method
Weighting scheme, w	$[\sigma^2(F) + 0.022(F)^2]^{-1}$	$6.9187/[\sigma^2(F) + 0.004(F)^2]$	$1.3048/[\sigma^2(F) + 0.001(F)^2]$	$2.1785/[\sigma^2(F) + 0.0014(F)^2]$
R	0.083	0.052	0.056	0.061
R'	0.078	0.059	0.057	0.060

* Details in common: crystal system, monoclinic; $\alpha = \gamma = 90°$; $T = 298$ K; Mo-Kα radiation (λ = 0.710 69 Å); ω–2θ scan mode; background measurement, stationary crystal–stationary counter at beginning and end of scan, each for 25% of total scan time.

Table 8 Atomic coordinates (× 10^4) for compound **4**

Atom	X/a	Y/b	Z/c	Atom	X/a	Y/b	Z/c
Os(1)	1343(2)	8157(1)	1329(1)	C(32)	2768(36)	6273(25)	364(30)
Os(2)	216(2)	6678(1)	1174(1)	O(32)	3379(27)	5811(19)	366(23)
Os(3)	1543(1)	6956(1)	113(1)	C(33)	1915(44)	7630(30)	−629(39)
Au	3261(1)	7445(1)	1595(1)	O(33)	2235(28)	8081(20)	−1040(24)
P	5051(10)	7284(6)	2382(9)	C(1A)	5313(35)	6842(23)	3534(29)
C	184(39)	7524(26)	191(34)	C(1B)	6424(49)	6844(33)	4096(43)
O	−707(25)	7814(19)	−397(22)	C(1C)	6572(53)	6440(38)	4880(46)
C(1)	−567(50)	8384(36)	−1006(43)	C(1D)	5803(58)	6083(39)	5094(29)
C(11)	133(57)	8766(41)	1311(48)	C(1E)	4820(55)	6087(36)	4472(47)
O(11)	−603(39)	9109(28)	1285(32)	C(1F)	4517(37)	6455(26)	3635(32)
C(12)	1660(50)	8963(38)	611(44)	C(2A)	5680(41)	6666(29)	1810(36)
O(12)	2140(36)	9474(27)	393(31)	C(2B)	5475(51)	6849(35)	952(45)
C(13)	2266(44)	8416(30)	2442(40)	C(2C)	5933(59)	6406(46)	364(51)
O(13)	2845(28)	8566(19)	3192(25)	C(2D)	6561(50)	5771(37)	885(48)
C(21)	−627(37)	6009(26)	425(33)	C(2E)	6764(63)	5651(45)	1717(61)
O(21)	−1193(33)	5532(24)	−139(29)	C(2F)	6387(44)	6057(32)	2343(39)
C(22)	−907(52)	7010(38)	1444(44)	C(3A)	5814(41)	8214(28)	2557(35)
O(22)	−1556(34)	7371(24)	1651(30)	C(3B)	6830(36)	8264(24)	2537(29)
C(23)	633(39)	5933(27)	2143(36)	C(3C)	7317(43)	8980(31)	2714(36)
O(23)	1062(33)	5537(25)	2786(30)	C(3D)	6872(44)	9638(31)	2799(37)
C(31)	744(43)	6357(30)	−825(38)	C(3E)	5830(47)	9615(34)	2854(41)
O(31)	232(33)	6034(24)	−1524(30)	C(3F)	5252(31)	8880(22)	2709(25)

ligand (LUMO). This results in a less-polar excited state. The stronger stabilisation of the ground state by solvents of increased polarity is apparent from the increased transition energies observed.

Experimental

Materials and Methods.—None of the compounds reported here is particularly air sensitive, but all reactions were carried out under an atmosphere of dry nitrogen. Products were separated in the air by thin-layer chromatography with plates coated with Merk Kieselgel $60F_{254}$ (0.25 mm thick). All solvents were dried over appropriate reagents and distilled prior to use. All chemicals, except where stated, were purchased from commercial sources and used as supplied. The compounds $[Os_3H_3(CO)_9(\mu_3\text{-}COMe)]$ [15] and $[Os_3H_3(CO)_9(\mu_3\text{-}CCl)]$ [2a] were prepared by literature methods. Proton NMR spectra were obtained on either Bruker WM250 or AM400 instruments at 20 °C using deuteriated solvents as lock and reference [$SiMe_4$ ($\delta = 0$)], infrared spectra on either Perkin-Elmer 983 or 1700 instruments, and mass spectra on a Kratos MS12 spectrometer with *ca.* 70 eV (1.12×10^{-17} J) ionising potential at 90–150 °C. Tris(perfluoroheptyl)-*s*-triazine was used as reference. Electronic absorption spectra were obtained in a microprocessor-

Table 9 Atomic coordinates (× 10^4) for compound **5**

Atom	*X/a*	*Y/b*	*Z/c*
Os(1)	3899(1)	984(1)	3729(1)
Os(2)	4047(1)	663(1)	1938(1)
Os(3)	2281(1)	−287(1)	2877(1)
C(1)	2177(20)	884(11)	2578(13)
N(1)	876(16)	1291(9)	2166(10)
C(100)	474(32)	1256(16)	1103(16)
C(101)	−1070(33)	1415(22)	758(19)
C(102)	−1613(27)	2084(16)	1121(17)
N(2)	−1215(17)	2058(10)	2136(12)
C(103)	−2225(30)	2487(17)	2608(17)
C(104)	−1456(37)	3100(18)	3214(29)
C(105)	−544(40)	2925(18)	4061(24)
C(106)	614(34)	2409(16)	4058(22)
C(107)	154(23)	1644(12)	3619(15)
C(108)	−73(19)	1667(10)	2603(12)
C(10)	3300(23)	1031(10)	4894(15)
O(10)	2998(20)	1090(9)	5586(11)
C(11)	4152(25)	2019(15)	3580(17)
O(11)	4330(24)	2644(10)	3526(15)
C(12)	6002(24)	806(11)	4212(15)
O(12)	7211(19)	753(11)	4450(13)
C(20)	4275(24)	1633(16)	1606(16)
O(20)	4390(21)	2270(9)	1343(13)
C(21)	6154(25)	382(15)	2134(14)
O(21)	7394(17)	267(10)	2304(13)
C(22)	3469(29)	286(16)	696(17)
O(22)	3224(23)	108(13)	−48(12)
C(30)	768(26)	−337(10)	3624(17)
O(30)	−101(21)	−357(12)	4076(14)
C(31)	879(27)	−564(12)	1810(22)
O(31)	13(22)	−728(9)	1221(15)
O(32)	3021(25)	−1280(13)	3220(17)
C(32)	3447(22)	−1865(9)	3421(17)

Table 10 Atomic coordinates (× 10^4) for compound **7**

Atom	*X/a*	*Y/b*	*Z/c*
Os(1)	6 254(1)	7 622(1)	7 839(1)
Os(2)	8 895(1)	8 703(1)	8 593(1)
Os(3)	6 268(1)	8 740(1)	9 087(1)
C(1)	7 514(19)	7 363(17)	8 830(9)
N	7 775(16)	6 271(12)	9 142(7)
C(2)	7 013(21)	6 022(17)	9 639(10)
C(3)	7 081(21)	4 997(17)	9 959(10)
C(4)	8 017(25)	4 199(20)	9 796(12)
C(5)	8 848(20)	4 384(15)	9 310(9)
C(6)	9 796(24)	3 562(20)	9 906(12)
C(7)	10 614(24)	3 794(19)	8 631(11)
C(8)	10 549(22)	4 849(18)	8 326(11)
C(9)	9 640(21)	5 632(16)	8 504(10)
C(10)	8 746(18)	5 465(14)	8 985(9)
C(11)	5 201(27)	8 338(22)	7 054(13)
O(11)	4 452(29)	8 791(17)	6 594(12)
C(12)	4 711(28)	6 591(23)	7 954(13)
O(12)	3 797(24)	5 968(18)	8 012(14)
C(13)	7 124(24)	6 538(20)	7 343(12)
O(13)	7 583(24)	5 863(18)	7 047(8)
C(21)	8 979(20)	10 267(18)	8 429(10)
O(21)	8 934(23)	11 243(12)	8 335(8)
C(22)	10 058(21)	8 794(15)	9 450(10)
O(22)	10 801(15)	8 814(11)	9 967(6)
C(23)	10 552(22)	8 270(17)	8 180(10)
O(23)	11 512(17)	8 039(15)	7 925(8)
C(31)	7 128(23)	8 838(17)	9 862(11)
O(31)	7 770(19)	8 857(15)	10 537(8)
C(32)	4 431(26)	8 169(19)	9 288(12)
O(32)	3 339(17)	7 811(17)	9 399(10)
C(33)	5 843(23)	10 368(20)	9 020(11)
O(33)	5 663(24)	11 290(13)	8 982(10)

Table 11 Atomic coordinates (× 10^4) for compound **9**

Atom	*X/a*	*Y/b*	*Z/c*
Os(1)	1784(1)	4925(2)	3548(1)
Os(2)	778(1)	5446(2)	2414(1)
Os(3)	1108(1)	2407(2)	3239(1)
C(1)	1242(9)	3743(32)	2411(16)
P	1263(3)	2975(12)	1625(6)
O(2)	1683(10)	1772(36)	1988(16)
C(2)	1784(18)	644(61)	1517(30)
O(3)	785(12)	2115(48)	982(21)
C(3)	435(19)	1894(68)	151(34)
O(4)	1303(16)	4160(45)	1079(26)
C(4)	1574(21)	5104(66)	933(34)
C(11)	1977(11)	6497(38)	3054(19)
O(11)	2078(10)	7499(34)	2772(17)
C(12)	2388(13)	3824(42)	4031(21)
O(12)	2767(9)	3140(38)	4308(18)
C(13)	1927(14)	6269(49)	4462(25)
O(13)	2020(10)	7045(37)	5031(17)
C(21)	837(14)	6931(51)	1764(24)
O(21)	889(11)	7996(36)	1396(20)
C(22)	131(13)	4798(41)	1512(21)
O(22)	−265(11)	4569(37)	909(18)
C(23)	669(11)	7026(42)	3056(20)
O(23)	647(12)	7878(30)	3463(18)
C(31)	1592(13)	717(42)	3515(21)
O(31)	1877(12)	−217(36)	3713(19)
C(32)	566(13)	1217(41)	2392(21)
O(32)	216(9)	530(34)	1840(17)
C(33)	987(13)	1805(45)	4095(23)
O(33)	992(10)	1478(36)	4679(14)

controlled Philips Analytical PU8000 spectrophotometer, thermostatted by a Haake F3-digital circulating bath.

Preparations.—$[N(PPh_3)_2][Os_3(\mu\text{-}H)_2(CO)_9(\mu_3\text{-}COMe)]$ **3**. The complex $[Os_3H_3(CO)_9(\mu_3\text{-}COMe)]$ **1** (100 mg, 0.1 mmol) was dissolved in CH_2Cl_2 (3 cm^3) and a dbu–CH_2Cl_2 solution (0.13 mmol) was added. The solution was left to stir at room temperature for 6 h. The solvent was removed *in vacuo* and the residue taken up in methanol (2 cm^3). Reduction of the volume gave yellow microcrystals of complex **3** (yield 135 mg, 87%).

$[Os_3(\mu\text{-}H)_2(\mu\text{-}AuPPh_3)(CO)_9(\mu_3\text{-}COMe)]$ **4**. Compound **3** (100 mg) was dissolved in CH_2Cl_2 (10 cm^3). A solution of $[Au(PPh_3)]Cl$ in CH_2Cl_2 (53 mg, 1.5 equivalents) was added dropwise using a pressure-equalised dropping funnel. The reaction mixture was left to stir at room temperature for 2 h. The solvent was evaporated to dryness and the residue chromatographed by TLC using hexane–CH_2Cl_2 (80:20) to give **4** as yellow microcrystals (yield 80 mg, 85%).

$[Os_3(\mu\text{-}H)_2(CO)_9(\mu_3\text{-}CN_2C_9H_{16})]$ **5**. The complex $[Os_3H_3(CO)_9(\mu_3\text{-}CCl)]$ **2** (50 mg) and $TlPF_6$ (30 mg) were stirred at room temperature. Addition of an excess of dbu (one drop) gave a yellow solution and an orange precipitate immediately. Separation of the yellow solution by TLC using hexane–CH_2Cl_2 (75:25) gave complex **5** as a yellow solid (yield 49 mg, 86%).

$[Os_3(\mu\text{-}H)_2(CO)_9(\mu_3\text{-}CNC_5H_5)]$ **6**. Pure compound **2** (100 mg, 0.11 mmol) and an excess of pyridine (three drops) were dissolved in CH_2Cl_2 (10 cm^3) and a dbu–CH_2Cl_2 solution (0.13 mmol) was added. The red reaction mixture was left to stir at room temperature for 30 min. Solvent was removed under vacuum and the red residue was chromatographed by TLC using hexane–CH_2Cl_2 (50:50) to afford complex **6** as a red powder (yield 66 mg, 63%).

$[Os_3(\mu\text{-}H)_2(CO)_9(\mu_3\text{-}CNC_9H_7)]$ **7**, $[Os_3(\mu\text{-}H)_2(CO)_9(\mu_3\text{-}CNC_9H_7)]$ **8** *and* $[Os_3(\mu\text{-}H)_2(CO)_9\{\mu_3\text{-}CP(OMe)_3\}]$ **9**. These compounds were synthesised using the conditions described for **6** with quinoline, isoquinoline and $P(OMe)_3$ as ligand respectively (yields *ca.* 65% for **7**, *ca.* 60% for **8** and *ca.* 40% for **9**).

Crystal Structure Analysis of Complexes **4**, **5**, **7** *and* **9**.—Table

7 summarises the relevant data for the crystal structure analyses. The unit-cell parameters were refined by a least-squares procedure. Three check reflections were monitored periodically throughout data collection and showed no significant variations. All intensity data were corrected for Lorentz polarisation effects, while absorption corrections by the ψ-scan method or a numerical method were applied for all compounds. The structures were solved by a combination of direct methods and Fourier difference techniques and refined on F by blocked full-matrix least-squares analysis (using the SHELXTL PLUS program).[16] The hydrogen atoms of the organic moieties were generated in their ideal positions (C–H 0.96 Å), while all metal hydride positions were estimated by potential-energy calculations.[17] Final atomic coordinates for the four structures are presented in Tables 8–11.

Additional material available from the Cambridge Crystallographic Data Centre comprises H-atom coordinates, thermal parameters and remaining bond lengths and angles.

Acknowledgements

We thank the Royal Commission for the Exhibition of 1851, the Committee of Vice-Chancellors and Principals of the Universities of the United Kingdom (W.-T. W), the SERC (N. D. P.) for financial support and the Ministerio de Education y Ciencia for a grant (to F. J. L.).

References

1 J. B. Keister, *Polyhedron*, 1988, **7**, 847; G. R. Frauenhoff, S. R. Wilson and J. R. Shapley, *Inorg. Chem.*, 1991, **30**, 78.
2 (*a*) J. B. Keister and T. L. Horling, *Inorg. Chem.*, 1980, **19**, 2304; (*b*) H. J. Kneuper, D. S. Strickland and J. R. Shapley, *Inorg. Chem.*, 1988, **27**, 1110.
3 J. Evans, P. M. Stroud and M. Webster, *Organometallics*, 1989, **8**, 1270.
4 D. K. Bower and J. B. Keister, *J. Organomet. Chem.*, 1986, **312**, C33; N. D. Prior, Ph.D. Thesis, University of Cambridge, 1988.
5 L. R. Beanan and J. B. Keister, *Organometallics*, 1985, **4**, 1713; L. R. Beanan, Z. A. Rahman and J. B. Keister, *Organometallics*, 1983, **2**, 1062.
6 T. P. Duggan, D. J. Barnett, M. J. Muscatella and J. B. Keister, *J. Am. Chem. Soc.*, 1986, **108**, 6076; M. R. Churchill, T. S. Janik, T. P. Duggan and J. B. Keister, *Organometallics*, 1987, **6**, 799.
7 L. W. Bateman, M. Green, K. A. Mead, R. M. Mills, I. D. Salter, F. G. A. Stone and P. Woodward, *J. Chem. Soc., Dalton Trans.*, 1983, 2599.
8 S. M. Owen, Ph.D. Thesis, University of Cambridge, 1989.
9 A. P. Humphries and H. D. Kaesz, *Prog. Inorg. Chem.*, 1979, **2**, 145.
10 M. R. Churchill and B. G. DeBoer, *Inorg. Chem.*, 1977, **16**, 878.
11 J. R. Shapley, D. S. Strickland, G. M. St. George, M. R. Churchill and C. Bueno, *Organometallics*, 1983, **2**, 185.
12 J. Evans and G. S. McNulty, *J. Chem. Soc., Dalton Trans.*, 1984, 79; J. B. Keister, M. W. Payne and M. J. Mucatella, *Organometallics*, 1983, **2**, 219; J. R. Shapley, M. E. Cree-Uchiyama, G. M. St. George, M. R. Churchill and C. Bueno, *J. Am. Chem. Soc.*, 1983, **105**, 140.
13 C. E. Housecroft, personal communication.
14 D. M. Mannta and A. J. Lees, *Inorg. Chem.*, 1986, **25**, 3212; W. Kaim, S. Kohlmann, S. Ernst, B. Olbrich-Deussner, C. Bessenbacher and A. Shulz, *J. Organomet. Chem.*, 1987, **321**, 215.
15 J. B. Keister, *J. Chem. Soc., Chem. Commun.*, 1979, 214.
16 G. M. Sheldrick, SHELXTL PLUS, An Integrated System for Solving, Refining and Displaying Crystal Structures from Diffraction Data, Göttingen, 1987.
17 A. G. Orpen, *J. Chem. Soc., Dalton Trans.*, 1980, 2509.

Received 16*th December* 1991; *Paper* 1/06311A